Investigation of neural stem cell biology in a mouse model of Rett syndrome

MAB Melone[1] T Squillaro[1], N Alessio[2], S Capasso[2], G Di Bernardo[2], M Cipollaro[2], G Peluso[3], U Galderisi[2]*

1.Department of Medical, Surgical, Neurological, Metabolic Sciences, and Aging; Division of Neurology and InterUniversity Center for Research in Neurosciences, University of Campania "Luigi Vanvitelli", Naples, Italy.
2.Department of Experimental Medicine, University of Campania "Luigi Vanvitelli", Naples, Italy.
3.Institute of Agro-Environmental Biology and Forestry (IBAF), CNR, Naples, Italy.
*4. * Author to whom correspondence should be addressed: marina.melone@unicampania.it; Tel.: +39-081-5666810*

Introduction

Epigenetics governs several aspects of stem cell life; changes in chromatin organization may be accountable for alterations in gene expression profile leading to senescence. The methyl-CpG-binding protein (MECP2) binds to methylated cytosines contributing to regulate gene expression [1]; mutations in MECP2 gene are present in up to 90% of Rett syndrome patients [2]. Nevertheless, the MECP2 role in this disease remains poorly understood. The MECP2 gene is ubiquitously expressed and its mutations can impair the function of many other genes in neural cells and in other tissues and organs, such as bones and muscles. Specifically, mutations of MECP2 can alter the activity of stem cells. This, in turn, can have a profound effect on the life of an individual. In a previous finding, we evidenced that mesenchymal stem cells (MSCs) obtained from Rett patients are prone to senescence [3]. Thus, we decided to investigate the effect of impaired MECP2 function on the *in vitro* behavior of neural stem cells (NSCs) obtained from a mouse model of Rett syndrome. This hypothesis took into consideration that in Rett syndrome patients present mainly neurological symptoms.

Methods

*H*eterozygous B6.129P2(C)-Mecp2tm1Bird/J females and the corresponding wild type mice were purchased from Jackson Laboratories. Animals were sacrificed to isolate and collect brains. NSCs were grown as neurospheres [4]. Neurospheres were mechanically dissociated and plated in DMEM/F12, B27 (ThermoFisher, Italy) without EGF and FGF2 onto poly-L-ornithine (Sigma-Aldrich Italy)-coated cell culture plates. Following differentiation induction [5], differentiated cells were identified by immunocytochemistry with a Neural Stem Cell Marker Characterization Kit (Millipore Italy). Cell growth was evaluated with the Quick Cell Proliferation Assay Kit II (Biovision, CA, USA). Cell cycle was analyzed by Guava EasyCyte flow cytometer (Merck Millipore, Italy). *A*poptosis was detected by means of fluorescein-conjugated Annexin V Kit (Roche, Italy). Trypan blue staining was used to identify necrotic non-viable cells. Senescence was evaluated with a quantitative, senescence-associated, beta-galactosidase assay, i.e. 4-Methylumbelliferyl-β-d-galactopyranoside (4-MUG). Western blot analysis was carried out to evaluate LC3, RB1, P21, P16, P53 protein expression levels. Immunocytochemistry for DNA repair proteins, i.e. ATM (Abcam), H2AX (Cell Signaling), RAD51 (Abcam) and DNA-PK (SantaCruz) following DNA damage induction by H_2O_2, UV and doxorubicin treatment was performed according to the manufacturers' instructions.

Results

The MTT proliferation assay revealed that the NSCs from mutated animals grew at a significant slower rate compared with those from control animals (Fig. 1D). In line with this result, in Mecp2+/- samples, we observed a reduction in the percentage of cells in S phase and stall in G2/M (Fig. 1B). Growth reduction was not coupled with changes in the percentage of apoptotic cells (Fig. 1C), rather with almost a doubling in the level of senescence (Fig. 1A). Reduction in cell growth and senescence onset were in agreement with an increase in the level of RB1, P16, and P21, which are part of cell cycle arrest and senescence-associated pathways (Fig. 2A) [6]. Of note, exit from the cell cycle and senescence were not related to P53 (Fig. 2A). We evaluated the autophagic flux in Mecp2+/- by determining the levels of two isoforms of the microtubule-associated protein 1 light chain 3 (LC3-I and LC3-II) [7]. We determined that the switch from LC3-I to LC3-II was impaired in NSCs obtained from mutated animals compared with controls (Fig. 2B). In Mecp2+/- samples we evidenced an increase in the number of cells with evident sign of damaged DNA (Fig. 3A). Following treatment with H_2O_2, NSCs from mutated animals showed a higher degree of apoptosis and necrosis with respect to control samples (Fig. 3B). This was associated with a significant increase in the mean number of H2AX foci per cells (Fig. 3A). Treatment with doxorubicin and UV produced the same outcomes. *Mecp2+/-* NSCs entered necrosis much more than control cells, while apoptosis was reduced and senescence unchanged (Fig. 3C-D). Moreover, in this case, we observed an increase in the percentage of cells with unrepaired or misrepaired DNA (Fig. 3A). In *Mecp2+/-* samples, we detected a significant reduction in the percentage of stem cells (8.6% vs 19.6%). We noticed an increase in the percentage of neurons (MAP2+) and the decrement of astrocytes (GFAP+) even though these trends were not statistically significant. Notably, we observed a massive increase (27.3% vs 1.6%) in the number of cells that were negative for both stem and differentiation markers. These may represent senescent cells that exited from correct neurogenesis processes (Fig. 4A and B).

Conclusions

Our research demonstrated that senescence of stem cell compartments may be associated with impaired function of Mecp2. It would be reasonable to set up anti-aging treatments in an animal model of the RTT disease. Our studies could pave the way to an innovative therapeutic approach to treating Rett syndrome.

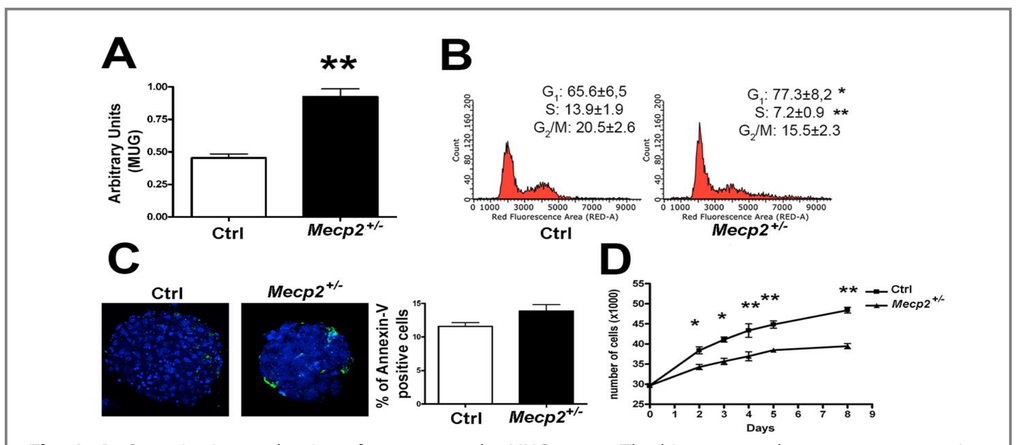

Fig. 1. A: Quantitative evaluation of senescence by MUG assay. The histograms shows mean expression values. **B:** Cell cycle analysis. A representative FACS analysis. **C:** Representative photomicrographs of apoptotic cells stained with Annexin V (green). Nuclei were counterstained with Hoechst 33342 (blue). The histograms shows mean expression values. **D:** Cell proliferation assay . At 2, 3, 4, 5 and 8 days post-plating, cells were collected and counted. (± SD, n = 3 biological replicates; *p < 0.05, **p < 0.01).

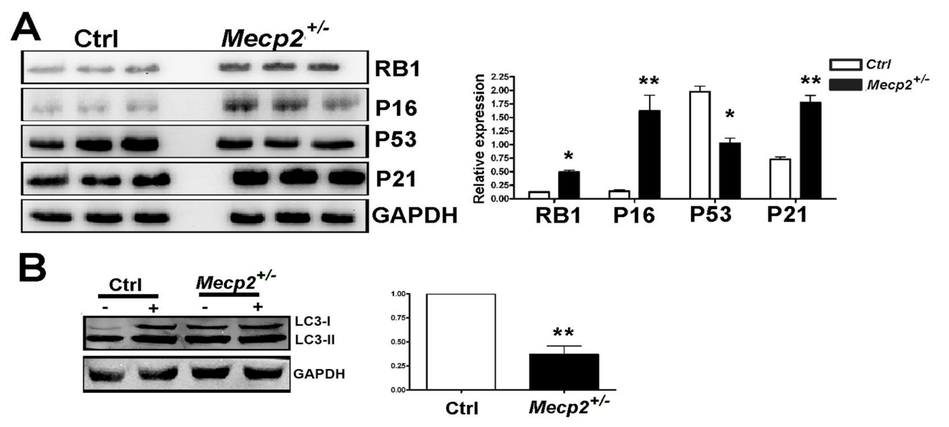

Fig. 2. A: The picture shows the expression levels of RB1, P16, P53 and P21 in Mecp2+/- and control samples. **B:** Western blot detection of LC3-I and LC3-II in Mecp2+/- and control NSCs. The detection of autophagic flux was performed by treating cultures with 100 nM of Bafilomycin A1 (+), an inhibitor of lysosomal degradation, or with PBS (-). Autophagy data are expressed in change folds. (± SD, n = 3 biological replicates; *p < 0.05, **p < 0.01).

Fig.3. A: Representative photos show the merging of cells stained with anti-H2AX (green) and DAPI (blue). The graph indicates the degree of H2AX phosphorylation that was determined by counting the number of gamma-H2AX immunofluorescent foci per cell. Each dot represents a single cell. Horizontal bars indicate mean value for each category (Mecp2+/- and control NSCs). DNA damage level following genotoxic treatments with H2O2, doxorubicin and UV irradiation, respectively. For every condition the degree of DNA damage was determined by counting gamma-H2AX foci.
B, **C** and **D**: Changes in the level of senescence, apoptosis and necrosis in Mepc2+/- NSCs compared to control cultures. Data are expressed in change folds (± SD, n = 3 biological replicates; *p < 0.05, **p < 0.01).

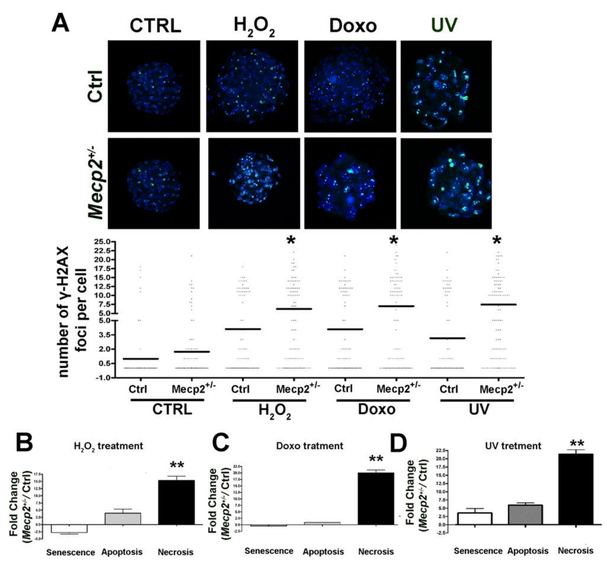

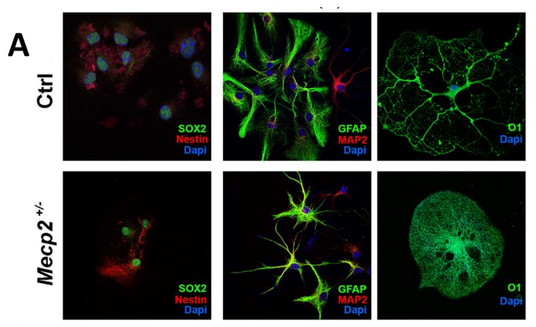

Fig.4. A: Representative photomicrographs of *Mecp2+/-* and control NSCs differentiated for 3 days onto poly-Lornithine- coated plates in medium without growth factors. Cells were stained for SOX2, Nestin, MAP-2, GFAP and O1. Nuclei were counterstained with DAPI. **B:** Percentages of stem cells (SOX2+; Nestin +), committed progenitors (SOX2+), neurons (MAP2+), astrocytes (GFAP+) and oligodendrocytes (O1+). Data were obtained from experiments depicted in A (n = 3 biological replicates; *p < 0.05, **p < 0.01).

B

	SOX2	SOX2 Nestin	MAP2	GFAP	O1	-
Ctrl	34.1±5.1	19.6±2.3	2.6±0.4	39.7±6.7	2.4±0.3	1.6±0.2
Mecp2+/-	26.0±4.1	8.6±0.9 **	6.2±1.0 *	29.7±3.8	2.2±0.4	27.3±4.6 **

Bibliography

1. Fuks F, Hurd PJ, Wolf D, Nan X, Bird AP, Kouzarides T. The methyl-CpG-binding protein MeCP2 links DNA methylation to histone methylation. J Biol Chem, 2003, 278(6): 4035-4040.
2. Kim HJ, Kim SH, Kim HD, Lee JS, Lee YM, Koo KY, Lee JS, Kang HC. Genetic and epileptic features in Rett syndrome. Yonsei Med J. 2012 May; 53(3):495-500.
3. Squillaro T, Hayek G, Farina E, Cipollaro M, Renieri A, Galderisi U. A case report: bone marrow mesenchymal stem cells from a Rett syndrome patient are prone to senescence and show a lower degree of apoptosis. Journal of cellular biochemistry 2008, 103(6): 1877-1885.
4. Bonaguidi MA, Peng CY, McGuire T, Falciglia G, Gobeske KT, Czeisler C and Kessler JA. Noggin expands neural stem cells in the adult hippocampus. The Journal of neuroscience: he official journal of the Society for Neuroscience 2008;28:9194-204
5. Jori FP, Galderisi U, Napolitano MA, Cipollaro M, Cascino A, Giordano A and Melone MA. RB and RB2/P130 genes cooperate with extrinsic signals to promote differentiation of rat neural stem cells. Molecular and cellular neurosciences 2007;34:299-309
6. Campisi J, d'Adda di Fagagna F. 2007. Cellular senescence: when bad things happen to good cells. Nature reviews. Molecular cell biology 8(9):729-740.
7. Mizushima N. Methods for monitoring autophagy. The international journal of biochemistry & cell biology 2004;36:2491-502.

Sin
XLVIII CONGRESSO NAZIONALE
14-17 OTTOBRE 2017 – NAPOLI
WebPoster
http://congress.wooky.it/NEURO2017/